



HAL
open science

Technical note: investigating activity-induced 3d hand enthesal variation in a documented South African sample

Lucile Bousquié, Fotios Alexandros Karakostis, Isabelle Crevecoeur, Sébastien Villotte

► To cite this version:

Lucile Bousquié, Fotios Alexandros Karakostis, Isabelle Crevecoeur, Sébastien Villotte. Technical note: investigating activity-induced 3d hand enthesal variation in a documented South African sample. *Archaeological and Anthropological Sciences*, 2022, 14 (11), pp.213. 10.1007/s12520-022-01677-1. hal-03859950

HAL Id: hal-03859950

<https://hal.science/hal-03859950>

Submitted on 25 Nov 2022

HAL is a multi-disciplinary open access archive for the deposit and dissemination of scientific research documents, whether they are published or not. The documents may come from teaching and research institutions in France or abroad, or from public or private research centers.

L'archive ouverte pluridisciplinaire **HAL**, est destinée au dépôt et à la diffusion de documents scientifiques de niveau recherche, publiés ou non, émanant des établissements d'enseignement et de recherche français ou étrangers, des laboratoires publics ou privés.



Technical note: investigating activity-induced 3d hand enthesal variation in a documented South African sample

Lucile Bousquié¹ · Fotios Alexandros Karakostis² · Isabelle Crevecoeur³ · Sébastien Villotte^{4,5}

Received: 24 January 2022 / Accepted: 20 September 2022 / Published online: 10 October 2022
© The Author(s) 2022

Abstract

For reconstructing physical activity in the past, the surfaces of bones where muscles and ligaments attach, “entheses,” are routinely studied. Previous research has introduced an experimentally validated virtual approach for reconstructing habitual activity based on entheses. The present study relies on this virtual method to further investigate the effects of various biological factors on entheses, including variation by ancestry. Our skeletal sample includes 39 individuals from the well-preserved Pretoria Bone Collection in South Africa. Although the size of the sample is limited, all selected individuals present excellently preserved left- and right-hand bones. Moreover, all individuals are reliably documented for sex, biological age, and ancestry (i.e., African or European origin). Multivariate analyses were run on both raw and size-adjusted hand enthesal three-dimensional measurements. Our findings showed that, after size adjustment, enthesal multivariate patterns did not significantly vary by sex, biological age, or estimated body mass. However, a significant (p -value=0.01) variation was found between individuals of different ancestries in only the right-hand side of our South African skeletal sample. The observed enthesal patterns were consistent with the habitual performance of power grasping in individuals of African origin, while our small sample’s European individuals showed distinctive indications of precision grasping behaviors. This pilot research provided important new insights into potentially activity-induced differences between population samples from South Africa, supporting the value of the applied protocol in reconstructing aspects of past human lifestyles. In the future, the functional interpretations of this study on interpopulation variation may be validated using increased sample sizes and individuals with long-term occupational documentation.

Keywords Muscle attachments · Ancestry · South Africa · “Validated Entheses-based Reconstruction of Activity (V.E.R.A.),” Virtual anthropology

Introduction

Reconstructing activity in the past is a major objective of biological anthropology. Researchers mostly follow the principle of “functional adaptation of the bone” (Lieberman and Friedlaender 2005; Ruff et al. 2006), according to which bone morphology can alter during life to ensure its endurance against changes in activity-induced strain (Ruff et al. 2006). On this basis, various skeletal proxies of physical activity have been proposed, such as cross-sectional geometric properties, trabecular architecture, or the bone surface areas where ligaments and/or muscles attach (often defined as “entheses”; e.g., Bennell et al. 1997; Benjamin et al. 2002; Benjamin et al. 2006; Vickerton et al. 2014; Kivell 2015; Dunmore et al. 2020). Similarly, other approaches have focused on the degenerative aspects of bone and studied osteoarthritis and/or enthesopathy (e.g., Cope et al. 2005;

✉ Fotios Alexandros Karakostis
fotios-alexandros.karakostis@uni-tuebingen.de

¹ Department of Anthropology, University of Montreal, Montreal, QC, Canada

² DFG (Deutsche Forschungsgemeinschaft) Center for Advanced Studies “Words, Bones, Genes, Tools”, Eberhard Karls University of Tübingen, Tübingen, Germany

³ CNRS, UMR 5199, PACEA, University of Bordeaux, Bordeaux, France

⁴ CNRS, UMR 7206 Éco-Anthropologie, University of Paris, Paris, France

⁵ Directorate Earth and History of Life, Royal Belgian Institute of Natural Sciences, Brussels, Belgium

Villotte and Knusel 2014; Molnar et al. 2011; Milella 2018; Laffranchi et al. 2020).

The most usual approaches for the study of enthesal changes are different scoring systems relying on visual observation of the enthesal expression and/or enthesopathy (Hawkey and Merbs 1995; Robb 1998; Stirland 1998; Mariotti et al. 2004, 2007; Villotte 2006; Villotte et al. 2010; Niinimäki 2011; Cashmore and Zakrzewski 2013; Weiss 2015; Kubicka and Myszka 2020), for the ultimate purpose of reconstructing physical activity in the past (e.g., Molnar 2010; Havelkova et al. 2011, 2013; Niinimäki 2012; Weiss et al. 2012). Nevertheless, several studies focusing explicitly on scoring enthesal changes have reported that these methods present issues of reproducibility (Davis et al. 2013; Henderson et al. 2016; Wilczak et al. 2017; Jorgensen et al. 2020). Other authors, such as Wilczak (1998) and Henderson (2013), used 2D measurements of entheses. With the recent advent of high-definition three-dimensional (3D) scanning, new methods of enthesal measurement were developed (e.g., Noldner and Edgar 2013). These were used to quantify enthesal 3D form and analyze it using complex and rigorous statistical analyses (Karakostis and Lorenzo 2016). Importantly, the latest developments in 3D scanning technologies using structured-light handheld models have greatly decreased the time required to generate high-resolution scans. For instance, the equipment used in the present study (see the section below) can provide a 3D model of a human hand bone within less than 5 minutes (including the process of texture mapping).

Most previous 3D studies rely on isolated entheses located in the upper limb (e.g., Noldner and Edgar 2013; Nolte and Wilczak 2013; Karakostis and Lorenzo 2016). Indeed, the upper limbs are the part of the skeleton that is expected to be the most impacted by repeated activity during life compared with the lower limbs or the axial skeleton (Cashmore and Zakrzewski 2013; 335). However, as some authors previously suggested, muscles act in coordination, and studying only isolated entheses leads to a substantial loss of functional information (Robb 1998; Stirland 1998; Henderson and Alves Cardoso 2012).

Recently, a new virtual approach for analyzing entheses was introduced, which involves the use of a detailed protocol for precise delineation and measurement of 3D enthesal surfaces (e.g., Karakostis and Lorenzo 2016; Karakostis et al. 2017, 2021). This is followed by multivariate analyses aiming to reconstruct patterns of habitual coordination among different muscles (i.e., synergies). This method, which was first developed by one of us in 2016 (author FAK; Karakostis and Lorenzo 2016), has recently been named the “Validated Entheses-based Reconstruction of Activity” (V.E.R.A.) method in a dedicated literature review (Karakostis and Harvati 2021). Its reliability has been validated both on human skeletons with long-term occupational

documentation (Karakostis et al. 2017) as well as in three experimental studies involving diverse laboratory animal species (Karakostis et al. 2019a, b; Castro et al. 2021). In particular, Karakostis and colleagues (2017) reported consistent differences between lifelong heavy manual laborers (presenting an enthesal pattern associated with a power-grasping muscle group) and long-term workers of lower intensity and/or more mechanized occupations (showing an enthesal pattern corresponding to a thumb-index precision-grasping muscle group). Importantly, these multivariate enthesal patterns were not associated with variation in biological age (all individuals were less than 50 years old, given the results of previous research showing the increase of pathological lesions at entheses after around this age and the decrease of a functional signal; e.g., see Mariotti et al. 2007; Villotte et al. 2010), body-size, or sex. Despite these promising findings, as highlighted by these authors themselves, further research is necessary for elucidating the exact effects of ancestry and sex on the multivariate patterns among entheses (Karakostis et al. 2020, 2021; Karakostis and Harvati 2021). Such studies are needed to address the applicability of the method V.E.R.A. for interpopulation comparisons, evaluating the method’s capacity to identify potential differences in habitual activity among individuals of diverse population origins.

In this framework, the present pilot study applied this novel methodology to the well-preserved hand bones of a small sample originating from the Pretoria Bone Collection (South Africa), which is reliably documented for the individuals’ sex, age at death, and ancestry (European or African).

Material and methods

Material

A total of 39 individuals from the Pretoria Bone Collection (PBC), South Africa, were analyzed for this research (L’Abbé et al. 2021). The PBC comprises more than 800 individual skeletons (body donors), who lived and died in the broader area of South Africa from 1942 onwards. Although the sample is arguably small, it represents individuals of known characteristics with excellently preserved left- and right-hand bones (a condition that is extremely rare among anthropological collections). The documentation of the PBC includes sex, body size, age at death, and ancestry. In this study, individuals of varying origins are referred to as either “South Africans with African ancestry” or “South Africans with European ancestry”. Reflecting previous applications of V.E.R.A. on hand entheses, the six following hand bones were analyzed for both anatomical sides (left and right): the first and fifth metacarpals (MTC1 and MTC5), the first, second, and fifth proximal phalanges (PP1;

PP2 and PP5), and the first distal phalanx (DP1). Considering the known impact of degenerative changes on enthesal morphology (Bloebaum and Kopp 2004; Milella et al. 2012; Nolte and Wilczak 2013; Villotte and Knusel 2013), individuals between 20 and 49 years at death were initially chosen from both sexes and ancestries. However, given the lack of individuals below 50 years of age in the PBC, individuals between 50 and 59 years of age at death were also included. Following the VERA protocols (Karakostis and Lorenzo 2016; see review by Karakostis and Harvati 2021), individuals with entheses showing potentially pathological lesions with more than 1 mm in diameter (either osteophytic or osteolytic; see Mariotti et al. 2004, 2007) were excluded from the sample. This decision was based on previous histological research showing that small enthesophytes (spurs) do not seem to compromise the microscopic bone-tendon interface in humans (Benjamin et al. 2001). These were extensive lesions of several mm in diameter, which appear to have resulted from post-traumatic bone remodeling. Depending on the analysis (see below) individuals were grouped by sex, ancestry, and the interaction between the two grouping factors (i.e., African ancestry females, African ancestry males, European ancestry females, and European ancestry males). Table 1 outlines the distribution of the sample, dividing individuals into arbitrary age groups for descriptive purposes. It should be clarified here that the statistical assessment of the effects of age on our results (see below) did not rely on any categorization into age groups, but instead used the exact documented age of each individual (see subsection “Statistical analysis”).

Table 1 Distribution of the 39 individuals of the sample

Ancestry	Sex	Age at death	Number of individuals	Total	
African	Females	20–29 years	3	12	
		30–39 years	3		
		40–49 years	3		
		50–59 years	3		
	Males	20–29 years	3		12
		30–39 years	3		
		40–49 years	3		
		50–59 years	3		
European	Females	20–29 years	2	8	
		30–39 years	0		
		40–49 years	3		
		50–59 years	3		
	Males	20–29 years	0		7
		30–39 years	1		
		40–49 years	3		
		50–59 years	3		

Delimitation and measurement of entheses

This paper employs the V.E.R.A. protocols for delineating enthesal areas on the bones, which were introduced in previous research (e.g., Karakostis and Lorenzo 2016; Karakostis et al. 2017, 2019a, b). The steps of this method are described in detail in a recent literature review by Karakostis and Harvati (2021). The first step involves the development of a 3D surface scan of each bone to be analyzed. An Artec 3D Space Spider scanner (Artec Inc., Luxembourg) was used together with the associated Artec Studio Professional 14 software. Then, each of the nine entheses located on the six bones was virtually isolated and their surfaces were measured in square millimeters with the Meshlab software (CNC Inc., Rome). Figure 1 shows the location of each enthesis and Table 2 explains the properties of each related muscle. Following V.E.R.A., to delineate and isolate the entheses, three criteria were used: the difference of elevation between the enthesal region and the rest of the surrounding bone, the difference in color shade, and the variation in surface complexity. This process is facilitated through the precise use of specific virtual tools (e.g., imaging filters). First the (optional) “equalize vertex color” filter permits to emphasize color differentiation on the bone surface. Then the “discrete curvatures” tool is used to color-map the elevation and complexity of the surface, allowing for the refinement of the delineation. Finally, after virtually selecting the enthesal area plus a narrow band of the surrounding flatter bone surface, the “compute curvatures principal directions” tool is used to precisely delineate the exact borders of the enthesal area and remove the surrounding flatter bone surface (see Karakostis and Lorenzo 2016; Karakostis and Harvati 2021). Finally, the remaining enthesal 3D area was measured in mm², using Meshlab’s measuring tools. For an observer experienced in the use of VERA, the above delineation process can be performed within 5 minutes for each enthesis (Karakostis and Harvati 2021). Table 3 presents the descriptive statistics for each enthesis, based on all 39 individuals. The intra-observer repeatability of this method of 3D delineation (VERA protocol) for this sample was tested for each enthesis using intra-observer tests. The first author (LB) executed twice the delineation of the left entheses of six individuals, which were randomly chosen among the sample. Then, a paired *t*-test between the first and the second 3D area measurements was run. In addition, the Lin’s concordance coefficient was also calculated to compare the measurements of the first session and the second one (following Lin 1989; Altman 1991; McBride 2005; Quinn et al. 2009).

Statistical analysis

Initially, to evaluate the potential effects of overall size in our analyses, our enthesal 3D area measurements (in mm²) were adjusted based on the geometric mean

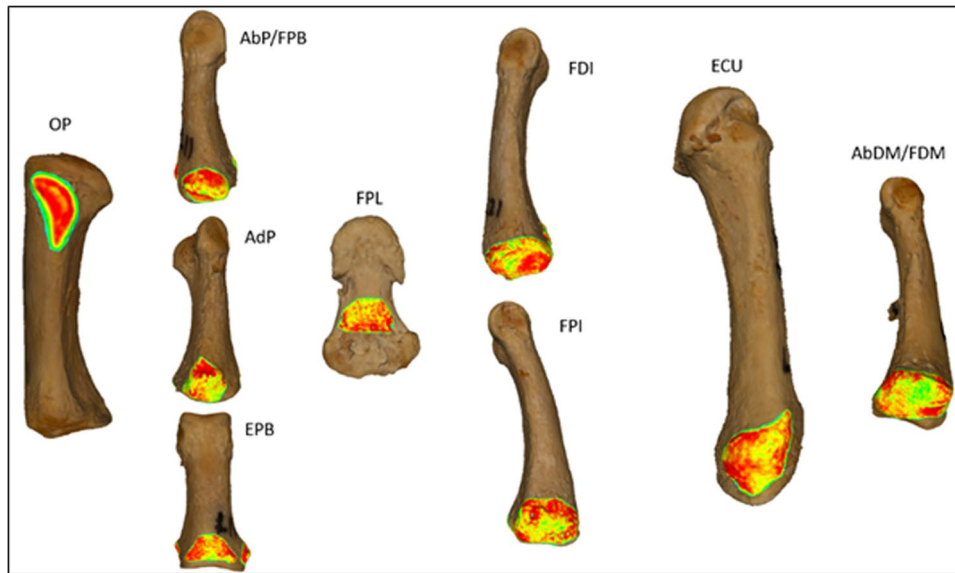


Fig. 1 The areas of the nine analyzed entheses located on the six hand bones, left side. Opponens pollicis (OP) on MTC1 (radial view); Abductor pollicis (AbP)*, Flexor pollicis brevis (FPB)*, Adductor pollicis (AdP) et Extensor pollicis brevis (EPB) on PP1 (from the top: radial, ulnar, and dorsal view); Flexor pollicis longus (FPL) on DP1 (palmar view); First dorsal interosseus (FDI) and First palmar interosseus (FPI) on PP2 (from the top: radial and ulnar view); Extensor

carpi ulnaris (ECU) on MTC5 (ulnar view); and Abductor digiti minimi (AbDM)* and Flexor digiti minimi (FDM)* on PP5 (ulnar view). The exact scale is not respected. *Those entheses were combined as the muscles insert in the same region of the bone, and thus individual delimitation per muscle attachment was not possible (for more details, see Karakostis and Lorenzo 2016; Karakostis et al. 2017)

Table 2 Properties of the analyzed entheses' muscles (Moore et al. 2014; Platzer 2014; Karakostis et al. 2017, 2019a)

Name of entheses associated muscles	Movement involved by the muscle	Bone where muscle inserts	Location of the enthesis on the bone
Opponens pollicis (OP)	Thumb opposition via flexion and abduction of the trapezio-metacarpal joint	MTC 1	Radial diaphysis
Abductor pollicis (AbP)	Thumb's abduction, assists in opposition	PP 1	Radial base
Flexor pollicis brevis (FPB)	Thumb's flexion, assists in opposition		Ulnar base
Adductor pollicis (AdP)	Thumb's adduction, assists in opposition		Dorsal base
Extensor pollicis brevis (EPB)	Thumb extension, assists in abduction		Palmar diaphysis
Flexor pollicis longus (FPL)	Thumb's flexion at the distal joint	DP 1	Radial base
First dorsal interosseus (FDI)	Second digit's abduction, assists in flexion	PP 2	Ulnar base
First palmar interosseus (FPI)	Second digit's adduction, assists in flexion		Ulnar base
Extensor carpi ulnaris (ECU)	Fifth digit's adduction and ulnar deviation	MTC 5	Ulnar base
Abductor digiti minimi (AbDM)	Fifth digit's abduction, assists in flexion	PP 5	Ulnar base
Flexor digiti minimi (FDM)	Fifth digit's flexion		

approach (e.g., Richmond et al. 2016) and following V.E.R.A.'s standard protocols (e.g., Karakostis et al. 2017, 2018, 2021). Subsequently, all statistical tests (see below) were applied both on raw as well as on size-adjusted enthesal 3D area measurements.

Assessing the effects of age and estimated body mass

The influence of estimated body mass on the enthesal patterns of individuals was analyzed with Spearman's

Table 3 Descriptive analysis of raw enthesal measurements (in mm²) based on all 39 individuals for each enthesis, right and left hand sides separated

		OP	AbP/FPB*	AdP	EPB	FPL	FDI	FPI	ECU	AbDM/FDM*
Mean	Left side	89.30	74.40	84.38	59.05	48.89	132.14	101.68	121.75	79.96
	Right side	92.28	80.65	91.95	61.64	46.45	137.52	98.87	125.15	84.36
Standard deviation	Left side	43.12	22.32	22.63	18.47	13.26	28.84	30.81	32.23	18.43
	Right side	31.26	22.10	32.55	19.57	12.10	27.14	26.12	30.34	18.84
Range	Left side	227.95	93.09	87.45	66.61	57.69	124.86	150.52	138.16	74.26
	Right side	127.91	101.75	165.23	90.99	42.63	96.35	122.74	107.65	95.08

*Those entheses were combined as the muscles insert in the same broader region of the bone, and thus individual delimitation per muscle attachment was not possible (for more details, see Karakostis and Lorenzo 2016; Karakostis et al. 2017)

correlation tests (r_s) involving the scores of the primary component of the principal component analysis (PCA; see subsection below). The process was repeated both for raw (unadjusted) and size-adjusted values (see below). We focused on the first principal component (PC1) because this axis showed different tendencies by ancestry (see plots in the “Results” section). In these comparisons, the femoral head diameter (measured in mm, using a Mitutoyo digital sliding caliper) was used as a proxy of body mass (see Ruff et al. 1991). Nevertheless, we have confirmed that either using femoral head diameters or predicted body mass values (calculated based entirely on the femoral head diameter as a single predictor variable) provided perfectly identical results in our correlation tests. Moreover, based on additional Spearman’s correlation tests, we estimated the influence of biological age on the observed enthesal patterns, by comparing between documented age and the PC1 of each PCA (before and after size-adjustment using the geometric mean approach).

Multivariate analysis of variance (MANOVA)

For investigating whether the observed enthesal differences between sexes and ancestries in our sample are statistically significant, a series of MANOVAs were applied on the raw 3D area measurements as well as on the data adjusted for overall size using the geometric mean approach. Initially, a comparison between males and females revealed that the size-adjusted dataset does not present significant sexual dimorphism in our sample’s left- and right-hand bones (see below, in the “Results” section). Based on this finding, and considering the admittedly limited size of our sample, the analyses focusing on ancestry relied on individuals from both sexes. All assumptions required for MANOVA were met, including the absence of outliers, approximate normality, and homogeneity of variance–covariance matrices (Field 2017). Outliers were identified and eliminated using the standard “z-score” approach (Field 2017). The approximate normality of the enthesal measurements was confirmed using histograms and normal probability plots

(Field 2017). Importantly, for each performed MANOVA, a Box’s M test confirmed the equality of variance–covariance matrices. To account for the possibility that multiple tests have increased the probability of a type I error, a Holm–Bonferroni sequential correction procedure was applied. Regarding sample size, the minimum recommended requirement was met (i.e., the number of individuals was greater than the number of independent factors; see Field 2017). In addition, we ensured that the *a priori* statistical power of all performed MANOVAs was adequate using the open-access software G*Power version 3.9.1.4 (Faul et al. 2007), which showed values well above 0.90 for all analyses (see the “Results” section) (Suresh and Chandrashekar 2012). The same software package was used to calculate effect sizes for all significant differences observed (Faul et al. 2007).

Principal component analyses (PCAs)

Considering the significant differences observed in the size-adjusted measurements of the right anatomical side (see the “Results” section), we used PCAs to investigate the multivariate patterns among entheses that lead to this ancestry-related variation in our sample. This analysis was performed in the software PAST (Hammer et al. 2001), relying on a correlation matrix.

A total of four PCAs were conducted (two for each anatomical side), involving raw and size-adjusted measurements (based on the geometric mean procedure; see above). The left and the right side were analyzed separately, to study the possible influence of activity impacting one side more than the other one. In all PCAs, the number of the PCs that were taken into account for each PCA was determined using standard scree plots in the software PAST (Field 2017). The entire sample was included in the analysis and individuals were color-labeled by ancestry. Therefore, all four PCAs conducted in this study did not assume groups *a priori*.

In the PCA on the size-adjusted dataset, all individuals showing extreme PC scores (i.e., above 3 or below –3) were excluded from the analyses (e.g., see Field 2017). After

excluding them and re-running the PCAs, one more case plotted slightly above 3 on PC2 (see Fig. 2). To fully ensure that this borderline extreme value did not considerably affect the distribution of individuals in the PCA plot and the associated PC loadings, we re-run the PCAs again without them. As the PCA patterns did not alter in any way, we maintained this very slightly extreme value in our plots (Fig. 2), to avoid further decreasing the small sample size of our study. Similarly, concerning the PCA on raw enthesal 3D values (i.e., before size adjustment), the analysis was re-run after removing 10 outliers. Nevertheless, some extreme values on PC2 re-emerged in the second analysis (see Fig. S1). As above, we confirmed that these extreme values did not considerably affect the observed PCA patterns (and statistical results) by re-running the PCAs without these extreme cases and repeating all correlation and comparison tests.

Results

Repeatability and the effects of age and estimated body mass

Table 4 presents the results of repeatability tests between the first and second series of measurements. All paired tests showed no significant differences between repetitions (p -values above 0.05), while the calculated Lin's concordance coefficient was 0.88, indicating adequate repeatability (see Lin 1989; Altman 1991).

Table 5 presents the results of the Spearman's correlation test between PC1 scores (from the PCA involving all individuals except outliers) and femoral head diameter (as a proxy of body mass). Before adjusting for size, the correlation between PC1 values and the femoral head diameter appears to be significant and relatively high. However, after size-adjusting the data based on the geometric mean approach, the femoral head diameter is no longer correlated with PC1 scores (p -values of 0.966 and 0.416). Table 6 presents the results of the same test, but this time comparing between PC1 and age-at-death. Once again, the PC1 relying on raw enthesal measurements shows a correlation with biological age in the left anatomical side. Nevertheless, size-adjusting the measurements based on the geometric mean appears to diminish the association between age-at-death and PC1 scores (p -values of 0.471 and 0.993).

MANOVA tests

Table 7 presents the results of the MANOVA tests comparing between sexes, for each anatomical side separately. Before size adjustment, the raw 3D enthesal values show a significant difference between sexes in the left anatomical side. The effect size for this difference (Cohen's f -squared) was calculated to be 1.52, indicating substantial mean variation between males and females (Faul et al. 2007). Nevertheless, once enthesal measurements were adjusted using the geometric mean, there were no statistically significant differences between sexes for either anatomical side.

Fig. 2 Plot of the first three PCs from the PCA based on 9 variables, right hand side (size adjusted enthesal measurements), and all individuals except for two extreme outliers (see the “Materials and Methods” section). African ancestry individuals labeled in dark blue and European ancestry individuals labeled in light blue. No groups were assumed *a priori* for this analysis

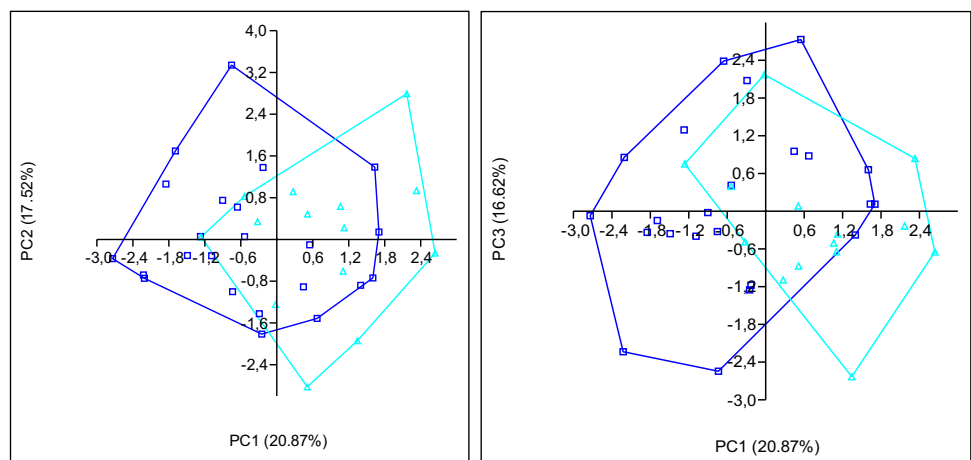


Table 4 Results of the intra-observer error tests, showing no significant differences between repetitions ($p > 0.05$)

Paired t -test	OP	AbP/FPB	AdP	EPB	FPL	FDI	FPI	ECU	AbDM/FDM
p -value	0.643	0.195	0.766	0.553	0.589	0.986	0.114	0.163	0.946
t	-0.493	-1.498	0.315	0.636	-0.577	0.019	-1.913	-1.635	-0.071

Table 5 Spearman correlation tests (r_s) between PC1 values and femoral head diameters used as a proxy of body mass

Raw or adjusted data	Side	r_s	p -value
Raw data	Left	0.539	0.003
	Right	0.665	< 0.001
Size-adjusted data	Left	-0.007	0.966
	Right	0.138	0.416

Adjusted data show no significant correlation whereas raw data do for both sides. Significant p -values are in bold

Table 6 Spearman correlation test (r_s) between PC1 values and age at death

Raw or adjusted data	Side	r_s	p -value
Raw data	Left	0.422	0.022
	Right	0.236	0.218
Size-adjusted data	Left	-0.120	0.471
	Right	0.002	0.993

Adjusted data show no significant correlation whereas raw data do for the left side. Significant p -values are in bold

Table 7 MANOVA test results comparing females and males of the sample

Raw or adjusted data	Side	Pillai trace	$df1$	$df2$	F	p -value	A priori statistical power
Raw data	Left	0.603	9	19	3.201	0.016	0.957
	Right	0.501	9	19	2.115	0.081	0.958
Size adjusted	Left	0.388	9	28	1.97	0.082	0.959
	Right	0.382	9	27	1.853	0.104	0.953

The data used in these analyses excluded 10 outliers for the raw data (left and right side pooled together), two outliers for the adjusted data of the right side, and one outlier for the adjusted data from the left side. The significant p -values (in bold) remained as such even after correcting using the Holm-Bonferroni sequential procedure

Table 8 MANOVA test results comparing between African ancestry and European ancestry individuals of the sample

Raw or adjusted data	Side	Pillai trace	$df1$	$df2$	F	p -value	A priori statistical power
Raw data	Left	0.485	9	19	1.988	0.099	0.961
	Right	0.327	9	19	1.024	0.457	0.952
Size adjusted	Left	0.351	9	28	1.686	0.140	0.956
	Right	0.512	9	27	3.171	0.010	0.966

The data used excluded 10 outliers for the raw data (left and right side together), two outliers for the adjusted data of the right side, and one outlier for the adjusted data from the left side. The significant p -value (in bold) remained as such even after correcting using the Holm-Bonferroni sequential procedure. The only significant difference between ancestries is observed in the size-adjusted values of the right anatomical side

Given this result, and to maximize our sample sizes for subsequent ancestry comparisons, we then pooled males and females together within each ancestry group. Table 8 displays the results of the tests comparing African and European ancestry individuals. In one of the comparisons, which focuses on the right-hand entheses, the difference is statistically significant (p -value: 0.01; see Field 2017). The effect size (Cohen’s f -squared) for that test was 1.05, indicating considerable deviation between the group means (Faul et al. 2007). Furthermore, the *a priori* statistical power of all comparisons is well above 0.90 (Suresh and Chandrashekhara 2012). It must be highlighted that this variation by ancestry in our sample only emerged when using the size-adjusted 3D surface areas. In contrast, these ancestry differences in our South African sample were not apparent when using the raw 3D surface measurements (i.e., prior to adjusting using the geometric mean).

Principal component analysis (PCA)

The PCAs conducted on the raw variables, whose components showed significant associations with biological age and femoral head diameter (Tables 5 and 6), are shown in the supplements (Fig. S1). Regarding the PCAs on size-adjusted measurements, Fig. 2 illustrates the PC scores of individuals when all nine enthesal measurements are included as

Table 9 Eigenvalues and factors loadings of the three PCAs

PCA	Principal Component	Eigen value	% of variance	Factor loadings										
				OP	AbP/FPB	AdP	EPB	FPL	FDI	FPI	ECU	AbDM/FDM		
African ancestry individuals and European ancestry individuals, raw data, left side (Figure S1)	PC1	5.18	57.61	0.26	0.35	0.37	0.30	0.37	0.34	0.35	0.28	0.37		
	PC2	1.10	12.25	0.63	-0.18	0.26	0.37	0.02	- 0.50	-0.20	0.08	-0.27		
African ancestry individuals and European ancestry individuals, raw data, right side (Figure S1)	PC1	4.50	50.00	0.25	0.36	0.36	0.34	0.35	0.36	0.33	0.29	0.37		
	PC2	1.06	11.78	0.77	-0.05	-0.01	-0.11	0.22	- 0.45	- 0.33	-0.01	0.18		
African ancestry individuals and European ancestry individuals, size adjusted, left side	PC1	2.14	23.74	-0.10	0.18	- 0.30	- 0.34	- 0.30	0.53	0.42	-0.12	0.43		
	PC2	1.81	20.07	- 0.65	-0.12	0.13	0.41	0.42	0.16	-0.03	-0.19	0.39		
	PC3	1.33	14.77	- 0.32	0.55	0.29	- 0.47	0.26	-0.03	-0.10	0.50	-0.02		
African ancestry individuals and European ancestry individuals, size adjusted, right side (Fig. 2)	PC1	1.88	20.87	-0.14	0.34	0.34	- 0.46	- 0.45	0.02	0.49	0.08	0.29		
	PC2	1.58	17.52	- 0.47	0.31	0.23	0.01	0.23	0.64	-0.22	- 0.33	-0.09		
	PC3	1.50	16.62	0.56	0.27	0.21	- 0.52	0.34	-0.14	-0.13	-0.25	- 0.30		

Loadings in bold are those above 0.3 and under -0.3

variables. Following the scree-plot approach, the first three PCs were plotted (see the “Materials and Methods” section). The plot shows the distribution of individual scores from both ancestries of our sample (based on right side, size-adjusted data). As mentioned before, no groups were assumed *a priori* for these analyses, but the individuals of each group were color-labeled differently for visualization purposes.

As shown in these plots (Fig. 2 left and right), most individuals of African ancestry tend to be mostly located on the negative side of the PC1. On the contrary, the PC1 scores of European ancestry individuals are mostly positive. Table 9, which presents the factor loadings for each principal component of the PCAs, shows that the positive values of PC1 represent individuals with proportionally larger AbP/FPB, AdP, and FPI (enthesal variables with a factor loading above 0.3), while negative values reflect proportionally larger EPB and FPL entheses (variables with loadings under -0.3).

Discussion

In line with previous works employing the V.E.R.A. approach (e.g., Karakostis and Lorenzo 2016; Karakostis and Harvati 2021), this study’s analyses suggest that size-adjustment combined with multivariate analysis of enthesal 3D areas can be used to adequately control for the effects of estimated body mass (Table 5), age-at-death (Table 6), and sexual dimorphism (Table 7) on muscle attachment surface areas. Conversely, before adjusting for size, these factors showed a significant effect on enthesal variation, confirming that the overall raw size of entheses (i.e., before adjustment) is naturally associated with the individual’s biological characteristics (e.g., Karakostis et al. 2017). On this basis, we encourage future 3D enthesal studies focusing on physical activity to consider the benefits of size adjustment and multivariate analysis.

Importantly, in our size-adjusted dataset, differences between ancestries (African and European) were statistically significant in our South African sample, explicitly for the enthesal multivariate patterns of the right-hand side. This difference is distinctive both in the statistical output of the MANOVA tests (Table 8) as well as in the PCA plots assuming no prior group differences (Fig. 2). Overall, these findings suggest that ancestry has a significant effect on the multivariate correlations among entheses in our small South African sample. Moreover, an observation of the PCA loadings (Table 9) suggests that this variation between individuals of different ancestries might be likely more driven by ancestry-based differences in habitual manual activities rather than genetic variation. In particular, Table 9 shows that the PC1 enthesal pattern of African ancestry individuals is mainly characterized by proportionally larger entheses of muscles

EPB and FPL. These muscles are known to be closely synergistic (e.g., Marzke et al. 1998; Karakostis and Lorenzo 2016), and their combined recruitment allows the thumb's proximal phalanx to extend back, while its distal phalanx flexes. Previous work has highlighted the importance of this interaction between muscles EPB and FPL for any power-grasping human gesture (Marzke et al. 1998; Karakostis et al. 2017). Similarly, the PC1 pattern of European ancestry individuals mainly involves entheses of a muscle group that tends to be typically vital for precision grasping (Moore et al. 2014; Kivell 2015; Karakostis et al. 2017). Particularly, the highest factor loadings were presented by the entheses of muscles AbP/FPB and AdP (Table 9), which are responsible for thumb abduction, adduction, and flexion. At the same time, entheses FPI and AbDM/FDM (which show lower factor loadings) correspond to muscles adducting the index finger and flexing and/or abducting the fifth ray, respectively. It is worth emphasizing that these enthesal differences by ancestry were also very similar within each sex separately and did not significantly correlate with biological age or femoral head diameter (a standard proxy of body mass).

Importantly, the possibility that variation by ancestry in our sample is driven by differences in habitual physical activity is also supported by the fact that only the right-hand side showed a significant difference between groups. This is even though both anatomical sides were perfectly preserved in all individuals of our sample. Essentially, if the observed differences were exclusively related to systemic factors of interindividual variability (such as genetic background), the results would not be expected to differ between the anatomical sides of the same individuals. Furthermore, the right side is typically more solicited during movement in most humans, given that most living humans are reported to be right-handed. Therefore, we could reasonably expect that, on a statistical basis, the right side might possibly be more influenced by the effects of activity compared to the left anatomical side (Steele and Mays 1995). In this regard, it is interesting to consider the historical context of this specific collection. The collection began accumulating in 1942, during the Apartheid period (L'Abbé et al. 2021). Many of the African ancestry individuals included in this collection were likely involved in strenuous manual and physical labor that was not as common among individuals of European ancestry, who also had access to a better health care system (e.g., Christopher 1990; Huschka and Mau 2006; Mariotti 2012; Natrass 2019). Our results on potential activity-induced skeletal differences between ancestries in our small South African sample may have likely identified a reflection of these social inequalities.

Despite the promising results of this pilot study, further research on increased sample sizes is required to validate our observations. Indeed, 39 individuals are evidently not representative of the entire South African population, nor of the

different ancestries included in it (L'Abbé et al. 2021; Alves Cardoso and Henderson 2013; Lopreno et al. 2013). Therefore, we would like to highlight as much as possible that our study's results and interpretations should never be generalized to all individuals of African and European ancestry, as they strictly refer to the sample of this study and its directly associated geo-chronological and historical context.

In the future, to further investigate the exact influence of other major factors of ancestry-based variability (e.g., genes), an adequate number of well-preserved and documented individuals from various ancestries and environmental contexts should be studied. It would also be important to include individuals with documented long-term occupational activities (e.g., see Karakostis et al. 2017). Overall, the findings of this study suggest that such future research endeavors would greatly benefit from employing the recently developed V.E.R.A. method (Karakostis and Lorenzo 2016; see review by Karakostis and Harvati 2021).

Conclusion

The present pilot study applied a recently developed and experimentally validated method of enthesal analysis (V.E.R.A. protocols) on a small but well-documented historical collection from South Africa, including individuals of African and European ancestry. After controlling for the effects of overall enthesal size, which was correlating with systemic factors (estimated body size, age-at-death, and biological sex), we found significant differences between ancestries in the right anatomical side. The observed enthesal differences appear to directly reflect the habitual performance of more strenuous manual activities in individuals of our sample with African ancestry. Future research on increased sample sizes is required to confirm these results and further elucidate the factors driving enthesal variation by ancestry.

Supplementary Information The online version contains supplementary material available at <https://doi.org/10.1007/s12520-022-01677-1>.

Acknowledgements The authors would like to thank Yann Heuzé (CNRS, UMR 5199, Pacea), Ericka l'Abbe (University of Pretoria), Gabi Krüger (University of Pretoria), Clarissa van der Merwe (University of Pretoria), and all the Bakeng se Afrika and Pacea team who made this research feasible.

Funding Open Access funding enabled and organized by Projekt DEAL. This research was funded by the Bakeng se Afrika program (Erasmus + and South Africa) as a collaboration between the University of Pretoria (South Africa) and the University of Bordeaux (France).

Declarations

Conflict of interest The authors declare no competing interests.

Open Access This article is licensed under a Creative Commons Attribution 4.0 International License, which permits use, sharing, adaptation, distribution and reproduction in any medium or format, as long as you give appropriate credit to the original author(s) and the source, provide a link to the Creative Commons licence, and indicate if changes were made. The images or other third party material in this article are included in the article's Creative Commons licence, unless indicated otherwise in a credit line to the material. If material is not included in the article's Creative Commons licence and your intended use is not permitted by statutory regulation or exceeds the permitted use, you will need to obtain permission directly from the copyright holder. To view a copy of this licence, visit <http://creativecommons.org/licenses/by/4.0/>.

References

- Alves Cardoso F, Henderson C (2013) The categorisation of occupation in identified skeletal collections: a source of bias? *Int J Osteoarchaeol* 23:186–196. <https://doi.org/10.1002/oa.2285>
- Altman D (1991) *Practical statistics for medical research*. Chapman and Hall, London
- Benjamin M, Kumai T, Milz S, Boszczyk B, Boszczyk A, Ralphs J (2002) The skeletal attachment of tendons—tendon ‘entheses.’ *Comp Biochem Physiol A* 133:931–945. [https://doi.org/10.1016/S1095-6433\(02\)00138-1](https://doi.org/10.1016/S1095-6433(02)00138-1)
- Benjamin M, Toumi H, Ralphs J, Bydder G, Best T, Milz S (2006) Where tendons and ligaments meet bone: attachment sites (‘entheses’) in relation to exercise and/or mechanical load. *J Anat* 208:471–490. <https://doi.org/10.1111/j.1469-7580.2006.00540.x>
- Benjamin M, Rufai A, Ralphs JR (2001) The mechanism of formation of bony spurs (enthesophytes) in the Achilles tendon. *Arthritis Rheum* 43(3):576–683
- Bennell K, Malcom S, Khan K, Thomas S, Ried S, Brukner P, Ebeling P, Wark J (1997) Bone mass and bone turnover in power athletes, endurance athletes, and controls: a 12-month longitudinal study. *Bone* 20(5):477–484. [https://doi.org/10.1016/S8756-3282\(97\)00026-4](https://doi.org/10.1016/S8756-3282(97)00026-4)
- Bloebaum R, Kopp D (2004) Remodeling capacity of calcified fibrocartilage of the hip. *Anat Rec* 279:736–739. <https://doi.org/10.1002/ar.a.20066>
- Castro A, Karakostis A, Copes E, McClendon E, Trivedi P, Schwartz E, Garland T (2021) Effects of selective breeding for voluntary exercise, chronic exercise, and their interaction on muscle attachment site morphology in house mice. *J Anat*. <https://doi.org/10.1111/joa.13547>
- Cashmore L, Zakrzewski S (2013) Assessment of musculoskeletal stress marker development in the hand. *Int J Osteoarchaeol* 23:334–347. <https://doi.org/10.1002/oa.1254>
- Christopher A (1990) Apartheid and urban segregation levels in South Africa. *Urban Studies* 27(3):421–440. <https://doi.org/10.1080/00420989020080361>
- Cope J, Berryman A, Martin D, Potts D (2005) Robusticity and osteoarthritis at the trapeziometacarpal joint in a Bronze Age population from Tell Abraq, United Arab Emirates. *Am J Phys Anthropol* 126:391–400. <https://doi.org/10.1002/ajpa.20097>
- Davis C, Shuler K, Danforth M, Herndon K (2013) Patterns of inter-observer error in the scoring of enthesal changes. *Int J Osteoarchaeol* 23:147–151. <https://doi.org/10.1002/oa.2277>
- Dunmore C, Bardo A, Skinner M, Kivell T (2020) Trabecular variation in the first metacarpal and manipulation in hominids. *Am J Phys Anthropol* 171:219–241. <https://doi.org/10.1002/ajpa.23974>
- Faul F, Erdfelder E, Lang G, Buchner A (2007) G*Power 3: a flexible statistical power analysis program for social behavioral, and biomedical sciences. *Behav Res Methods* 39(2):175–191. <https://doi.org/10.3758/bf03193146>
- Field A (2017) *Discovering statistics using IBM SPSS statistics*: North, American. Sage Publication, New-York
- Hammer O, Harper D, Paul R (2001) Past: paleontological statistics software package for education and data analysis. *Palaeontol Electron* 4(1):1–9
- Havelkova P, Villotte S, Veleminsky P, Polacek L, Dobisikova M (2011) Enthesopathies and activity patterns in the early Medieval Great Moravian population: evidence of division of labour. *Int J Osteoarchaeol* 21:487–504. <https://doi.org/10.1002/oa.1164>
- Havelkova P, Hladik M, Veleminsky P (2013) Enthesal Changes: do they reflect socioeconomic status in the Early Medieval Central European Population? (Mikulcice – Klásterisko, Great Moravian Empire, 9th – 10th century). *Int J Osteoarchaeol* 23:237–251. <https://doi.org/10.1002/oa.2294>
- Hawkey D, Merbs C (1995) Activity-induced musculo skeletal stress markers (MSM) and subsistence strategy changes among ancient Hudson Bay Eskimos. *Int J Osteoarchaeol* 5:324–338. <https://doi.org/10.1002/oa.1390050403>
- Henderson C, Alves Cardoso F (2012) Special issue enthesal changes and occupation: technical and theoretical advances and their applications. *Int J Osteoarchaeol* 23:127–134. <https://doi.org/10.1002/oa.2298>
- Henderson C (2013) Technical note: quantifying size and shape of entheses. *Anthropol Sci* 121(1):63–73. <https://doi.org/10.1537/ase.121017>
- Henderson C, Mariotti V, Pany-kucera D, Villotte S, Wilczak C (2016) The new “Coimbra method”: a biologically appropriate method for recording specific features of fibrocartilaginous enthesal changes. *Int J Osteoarchaeol* 26(5):925–932. <https://doi.org/10.1002/oa.2477>
- Huschka D, Mau S (2006) Social anomie and racial segregation in South Africa. *Soc Indic Res* 76:467–498. <https://doi.org/10.1007/s11205-005-2903-x>
- Jorgensen K, Mallon L, Kranioti E (2020) Testing interobserver and intraobserver agreement of the original and revised Coimbra methods. *Int J Osteoarchaeol* 30:769–777. <https://doi.org/10.1002/oa.2907>
- Karakostis A, Lorenzo C (2016) Morphometric patterns among the 3D surface areas of human hand entheses. *Am J Phys Anthropol* 160:694–707. <https://doi.org/10.1002/ajpa.22999>
- Karakostis A, Hotz G, Scherf H, Wahl J, Harvati K (2017) Occupational manual activity is reflected on the patterns among hand entheses. *Am J Phys Anthropol* 164:30–40. <https://doi.org/10.1002/ajpa.23253>
- Karakostis A, Hotz G, Tourloukis V, Harvati K (2018) Evidence for precision grasping in Neandertal daily activities. *Sci Adv* 4(9):1–11. <https://doi.org/10.1126/sciadv.aat2369>
- Karakostis A, Wallace I, Konow N, Harvati K (2019a) Experimental evidence that physical activity affects the multivariate associations among muscle attachments (entheses). *J Exp Biol* 222(23):1–24. <https://doi.org/10.1242/jeb.213058>
- Karakostis A, Jeffery N, Harvati K (2019b) Experimental proof that multivariate patterns among muscle attachments (entheses) can reflect repetitive muscle use. *Sci Rep* 9:1–9. <https://doi.org/10.1038/s41598-019-53021-8>
- Karakostis A, Reyes-Centeno H, Franken M, Hotz G, Rademaker K, Harvati K (2020) Biocultural evidence of precise manual activities in an Early Holocene individual of the high-altitude Peruvian Andes. *Am J Phys Anthropol* 241:1–14. <https://doi.org/10.1002/ajpa.24160>
- Karakostis A, Haeufle D, Anastopoulou I, Moraitis K, Hotz G, Tourloukis V, Harvati K (2021) Biomechanics of the human thumb and the evolution of dexterity. *Curr Biol* 31:1–9. <https://doi.org/10.1016/j.cub.2020.12.041>
- Karakostis A, Harvati K (2021) New horizons in reconstructing past human behavior: introducing the “Tübingen University Validated Entheses-based Reconstruction of Activity” method. *Evol Anthropol* 30(3):1–14. <https://doi.org/10.1002/evan.21892>
- Kivell T (2015) Evidence in hand: recent discoveries and the early evolution of human manual manipulation. *Philos Trans R Soc Publish* 370:1–11. <https://doi.org/10.1098/rstb.2015.0105>
- Kubicka A, Myszk A (2020) Are enthesal changes and cross-sectional properties associated with the shape of the upper limb?

- Am J Phys Anthropol 173:293–306. <https://doi.org/10.1002/ajpa.24096>
- L'Abbé E, Krüger G, Theye C, Hagg A, Sapo O (2021) The pretoria bone collection: a 21st century skeletal collection in South Africa. *Forensic Sci* 1:220–227. <https://doi.org/10.3390/forensicsci1030020>
- Laffranchi Z, Charisi D, Jimenez-Brobeil S, Milella M (2020) Gendered division of labor in a Celtic community? A comparison of sex differences in enthesal changes and long bone shape and robusticity in the pre-Roman population of Verona (Italy, third–first century BC). *Am J Phys Anthropol* 173:568–588. <https://doi.org/10.1002/ajpa.24111>
- Lieberman J, Friedlaender G (2005) Bone regeneration and repair: biology and clinical applications. Humana Press Inc, New-York
- Lin L (1989) A concordance correlation coefficient to evaluate reproducibility. *Biometrics* 45:255–268. <https://doi.org/10.2307/2532051>
- Lopreno G, Cardoso F, Assis S, Milella M, Speith N (2013) Categorization of occupation in documented skeletal collections: its relevance for the interpretation of activity-related osseous changes. *Int J Osteoarchaeol* 23:175–185. <https://doi.org/10.1002/oa.2301>
- Mariotti V, Facchini F, Belcastro M (2004) Enthesopathies – proposal of a standardized scoring method and applications. *Coll Antropol* 28(1):145–159
- Mariotti V, Facchini F, Belcastro M (2007) The study of entheses: proposal of a standardised scoring method for twenty-three entheses of the post-cranial skeleton. *Coll Antropol* 31(1):291–313
- Mariotti M (2012) Labour markets during apartheid in South Africa. *Econ Hist Rev* 65(3):1100–1122. <https://doi.org/10.1111/j.1468-0289.2011.00621.x>
- Marzke M, Toth N, Schick K, Reece S, Steinberg B, Hunt K, Linscheid R, An K (1998) EMG study of hand muscle recruitment during hard hammer percussion manufacture of oldowan tools. *Am J Phys Anthropol* 105:315–332. [https://doi.org/10.1002/\(SICI\)1096-8644\(199803\)105:3%3c315::AID-AJPA3%3e3.0.CO;2-Q](https://doi.org/10.1002/(SICI)1096-8644(199803)105:3%3c315::AID-AJPA3%3e3.0.CO;2-Q)
- Mcbride G (2005) A proposal for strength-of-agreement criteria for Lin's concordance correlation coefficient. *NIWA Rep* 62:1–14
- Milella M, Belcastro M, Zollikofer C, Mariotti V (2012) The effect of age, sex, and physical activity on enthesal morphology in a contemporary Italian skeletal collection. *Am J Phys Anthropol* 148:379–388. <https://doi.org/10.1002/ajpa.22060>
- Milella M (2018) Osteoarthritis/degenerative joint disease. In: Treva-than W (ed) *The international encyclopedia of biological anthropology*. John Wiley & Sons Inc, New-York
- Molnar P (2010) Patterns of physical activity and material culture on Gotland, Sweden, during the Middle Neolithic. *Int J Osteoarchaeol* 20:1–14. <https://doi.org/10.1002/oa.1000>
- Molnar P, Ahlstrom T, Leden I (2011) Osteoarthritis and activity—an analysis of the relationship between eburnation, musculoskeletal stress markers (MSM) and age in two Neolithic hunter–gatherer populations from Gotland, Sweden. *Int J Osteoarchaeol* 21:283–291. <https://doi.org/10.1002/oa.1131>
- Moore K, Dalley A, Agur A (2014) *Clinically oriented anatomy*. Lippincott Williams and Wilkins, Baltimore
- Natrass G (2019) *A short history of South Africa*. Jonathan Ball Publishers, Johannesburg
- Niinimäki S (2011) What do muscle marker ruggedness scores actually tell us? *Int J Osteoarchaeol* 21:292–299. <https://doi.org/10.1002/oa.1134>
- Niinimäki S (2012) The relationship between musculoskeletal stress markers and biomechanical properties of the humeral diaphysis. *Am J Phys Anthropol* 147:618–628. <https://doi.org/10.1002/ajpa.22023>
- Noldner L, Edgar H (2013) Technical note: 3D representation and analysis of enthesal morphology. *Am J Phys Anthropol* 152:417–424. <https://doi.org/10.1002/ajpa.22367>
- Nolte M, Wilczak C (2013) Three-dimensional surface area of the distal biceps enthesis, relationship to body size, sex, age and secular changes in a 20th century American sample. *Int J Osteoarchaeol* 23:163–174. <https://doi.org/10.1002/oa.2292>
- Platzer W (2014) *Atlas de poche d'anatomie : 1) Appareil locomoteur*. Lavoisier Médecine sciences, Stuttgart
- Quinn C, Haber M, Pan Y (2009) Use of the concordance correlation coefficient when examining agreement in dyadic research. *Nurs Res* 58(5):368–373. <https://doi.org/10.1097/NNR.0b013e3181b4b93d>
- Richmond B, Roach N, Ostrofsky K (2016) Chapter 18: Evolution of the early hominin hand. In: Kivell T, Lemelin P, Richmond B, Schmitt D (ed). *The evolution of the primate hand: anatomical, developmental, functional, and paleontological evidence*. Springer, New-York
- Robb J (1998) The interpretation of skeletal muscle sites: a statistical approach. *Int J Osteoarchaeol* 8:363–377. [https://doi.org/10.1002/\(SICI\)1099-1212\(199809\)8:5%3c363::AID-OA438%3e3.0.CO;2-K](https://doi.org/10.1002/(SICI)1099-1212(199809)8:5%3c363::AID-OA438%3e3.0.CO;2-K)
- Ruff C, Scott W, Liu A (1991) Articular and diaphyseal remodeling of the proximal femur with changes in body mass in adults. *Am J Phys Anthropol* 86:397–413. <https://doi.org/10.1002/ajpa.1330860306>
- Ruff C, Holt B, Trinkaus E (2006) Who's afraid of the big bad wolf? : “Wolff's Law” and bone functional adaptation. *Am J Phys Anthropol* 129:484–498. <https://doi.org/10.1002/ajpa.20371>
- Sirland A (1998) Musculo skeletal evidence for activity: problems of evaluation. *Int J Osteoarchaeol* 8:354–362. [https://doi.org/10.1002/\(SICI\)1099-1212\(199809\)8:5%3c354::AID-OA432%3e3.0.CO;2-3](https://doi.org/10.1002/(SICI)1099-1212(199809)8:5%3c354::AID-OA432%3e3.0.CO;2-3)
- Suresh P, Chandrashekar S (2012) Sample size estimation and power analysis for clinical research studies. *J Human Reprod Sci* 5(1):7–12
- Steele J, Mays S (1995) Handedness and directional asymmetry in the long bones of the human upper limb. *Int J Osteoarchaeol* 5:39–49. <https://doi.org/10.1002/oa.1390050105>
- Vickerton P, Jarvis J, Gallagher J, Akhtar R, Sutherland H, Jeffery N (2014) Morphological and histological adaptation of muscle and bone to loading induced by repetitive activation of muscle. *Proc R Soc* 281:1–9. <https://doi.org/10.1098/rspb.2014.0786>
- Villotte S (2006) Connaissances médicales actuelles, cotation des enthésopathies : nouvelle méthode. *Bull Mém Soc Anthropol Paris* 18(1–2):65–85. <https://doi.org/10.4000/bmsap.1325>
- Villotte S, Castex D, Couailler V, Dutour O, Knusel C, Henry-gambier D (2010) Enthesopathies as occupational stress markers: evidence from the upper limb. *Am J Phys Anthropol* 142:224–234. <https://doi.org/10.1002/ajpa.21217>
- Villotte S, Knusel C (2013) Understanding enthesal changes: definition and life course changes. *Int J Osteoarchaeol* 23:135–146. <https://doi.org/10.1002/oa.2289>
- Villotte S, Knusel C (2014) “I sing of arms and of a man”: medial epicondylitis and the sexual division of labour in prehistoric Europe. *J Archaeol Sci* 43:168–174. <https://doi.org/10.1016/j.jas.2013.12.009>
- Weiss E, Corona L, Schultz B (2012) Sex differences in musculoskeletal stress markers: problems with activity pattern reconstructions. *Int J Osteoarchaeol* 22:70–80. <https://doi.org/10.1002/oa.1183>
- Weiss E (2015) Examining activity patterns and biological confounding factors: differences between fibrocartilaginous and fibrous musculoskeletal stress markers. *Int J Osteoarchaeol* 25:281–288. <https://doi.org/10.1002/oa.2290>
- Wilczak C (1998) Consideration of sexual dimorphism, age and asymmetry in quantitative measurements of muscle insertion sites. *Int J Osteoarchaeol* 8:311–325. [https://doi.org/10.1002/\(SICI\)1099-1212\(199809\)8:5%3c311::AID-OA443%3e3.0.CO;2-E](https://doi.org/10.1002/(SICI)1099-1212(199809)8:5%3c311::AID-OA443%3e3.0.CO;2-E)
- Wilczak C, Mariotti V, Pany-kucera D, Villotte S, Henderson C (2017) Training and interobserver reliability in qualitative scoring of skeletal sample. *J Archaeol Sci Rep* 11:69–79. <https://doi.org/10.1016/j.jasrep.2016.11.033>

Publisher's note Springer Nature remains neutral with regard to jurisdictional claims in published maps and institutional affiliations.